European Heart Journal (2011) **32**, 294–304
doi:10.1093/eurheartj/ehq458

FASTTRACK

A comparative assessment by optical coherence tomography of the performance of the first and second generation of the everolimus-eluting bioresorbable vascular scaffolds

Josep Gomez-Lara[1†], Salvatore Brugaletta[1], Roberto Diletti[1], Scot Garg[1], Yoshinobu Onuma[1], Bill D. Gogas[1], Robert Jan van Geuns[1], Cécile Dorange[2], Susan Veldhof[2], Richard Rapoza[2], Robert Whitbourn[3], Stephan Windecker[4], Hector M. Garcia-Garcia[1], Evelyn Regar[1], and Patrick W. Serruys[1*†]

[1]Department of Interventional Cardiology, Ba583a, Thoraxcenter, Erasmus MC,'s-Gravendijkwal 230, 3015 CE Rotterdam, The Netherlands; [2]Abbott Vascular, Diegem, Belgium; [3]St Vincent's Hospital, Melbourne, Australia; and [4]Swiss Cardiovascular Centre, Bern, Switzerland

Received 8 September 2010; revised 28 October 2010; accepted 18 November 2010; online publish-ahead-of-print 1 December 2010

Aims The first generation of the everolimus-eluting bioresorbable vascular scaffold (BVS 1.0) showed an angiographic late loss higher than the metallic everolimus-eluting stent Xience V due to scaffold shrinkage. The new generation (BVS 1.1) presents a different design and manufacturing process than the BVS 1.0. This study sought to evaluate the differences in late shrinkage, neointimal response, and bioresorption process between these two scaffold generations using optical coherence tomography (OCT).

Methods and results A total of 12 lesions treated with the BVS 1.0 and 12 selected lesions treated with the revised BVS 1.1 were imaged at baseline and 6-month follow-up with OCT. Late shrinkage and neointimal area (NIA) were derived from OCT area measurements. Neointimal thickness was measured in each strut. Strut appearance has been classified as previously described. Baseline clinical, angiographic, and OCT characteristics were mainly similar in the two groups. At 6 months, absolute and relative shrinkages were significantly larger for the BVS 1.0 than for the BVS 1.1 (0.98 vs. 0.07 mm^2 and 13.0 vs. 1.0%, respectively; $P = 0.01$). Neointimal area was significantly higher in the BVS 1.0 than in the BVS 1.1 (in-scaffold area obstruction of 23.6 vs. 12.3%; $P < 0.01$). Neointimal thickness was also larger in the BVS 1.0 than in the BVS 1.1 (166.0 vs. 76.4 μm; $P < 0.01$). Consequently, OCT, intravascular ultrasound, and angiographic luminal losses were higher with the BVS 1.0 than with the BVS 1.1. At 6 months, strut appearance was preserved in only 2.9% of the BVS 1.0 struts, but remained unchanged with the BVS 1.1 indicating different state of strut microstucture and/or their reflectivity.

Conclusion The BVS 1.1 has less late shrinkage and less neointimal growth at 6-month follow-up compared with the BVS 1.0. A difference in polymer degradation leading to changes in microstructure and reflectivity is the most plausible explanation for this finding.

Keywords Bioresorbable vascular scaffold • Shrinkage • Optical coherence tomography • Bioresorption

Background

The first generation of the everolimus-eluting bioresorbable vascular scaffold (BVS 1.0) was tested in 30 patients enrolled in the ABSORB Cohort A study. At 6-month follow-up, this device showed a late shrinkage of the scaffold area of 11.8% as assessed by intravascular ultrasound (IVUS) and rapid changes in strut appearance, documented by multiple imaging modalities.[1]

† J.G.-L. and P.W.S. have equally contributed to the writing of the manuscript.

* Corresponding author. Tel: +31 10 7035260, Fax: +31 10 4369154, Email: p.w.j.c.serruys@erasmusmc.nl

At variance with metallic stents, which do not exhibit late shrinkage,[2] the reduction of the BVS 1.0 scaffold area was the main component of late luminal loss at 6 months.

The BVS 1.1 represents a new generation of bioresorbable devices. It utilizes a novel platform design and polymer processing different than the previous BVS 1.0. This new generation is designed to improve the radial force and to slow-down the loss in mechanical integrity, without substantially affecting the bioresorption process.[3] It has been investigated in 101 patients enrolled in the ABSORB cohort B trial. Forty-five of these patients were scheduled for a 6-month control with conventional angiography and multiple intravascular imaging techniques.

Optical coherence tomography (OCT) is a high resolution imaging technique capable of an accurate assessment of the polymeric struts, changes in luminal and scaffold dimensions, and the quantification of neointimal hyperplasia.[4–6]

Our aim is to compare the late shrinkage and neointimal response of the two polymeric devices using OCT imaging and to assess the qualitative changes in strut appearance as a marker of bioresorption at 6-month follow-up.

Materials and methods

Study design and population

The ABSORB trial is a non-randomized, multicentre, single-arm, efficacy–safety study. The first Cohort (A) included 30 patients treated with the BVS 1.0; the trial design and results up to 3-year follow-up have been already published.[1,4,7] The second Cohort (B) included 101 patients with 102 lesions treated with a single size 3 × 18 mm of the BVS 1.1 design; the study design is available at *clinicaltrials.gov* (NCT00856856).

The inclusion criteria were similar in both studies: patients aged 18 years or older diagnosed with stable, unstable, or silent ischaemia, with a *de novo* lesion in a native coronary artery between 50 and 99% of the luminal diameter and a Thrombolysis In Myocardial Infarction (TIMI) flow grade of 1 or more. Exclusions included patients with an evolving myocardial infarction, stenosis of an unprotected left main or ostial right coronary artery (RCA), presence of intracoronary thrombus or heavy calcification. Excessive tortuosity and lesions involving a side branch more than 2 mm in diameter were also exclusion criteria. The ethics committee at each participating institution approved the protocol and each patient gave written informed consent before inclusion.

Four centres (Auckland, Aarhus, Krakow, and Rotterdam) participated in the Absorb Cohort A in 2006 using the BVS 1.0.[1] In this first-in-man study, angiography and IVUS were mandatory investigations at 6 and 24 months of follow-up. Optical coherence tomography was an optional investigation that was only executed and performed in Rotterdam with the available system at that time (M2 Light Lab). Subsequently, the Rotterdam group performed OCT follow-up of their patients at 6 and 24 months. As a result, 13 patients in Cohort A had sequential OCT investigation at baseline and 6 months.[4] The Cohort B study was started during 2009 using the BVS 1.1. In this study, 7 of the 12 participating centres performed OCT at baseline and follow-up and three of them (Rotterdam = 9, Melbourne = 2, and Bern = 1) used the most advanced system (C7 Light Lab). As a result, 12 patients in Cohort B have been imaged with the OCT C7 system. This limited but almost equal number of patients represents a unique opportunity to analyse, with the high resolution of OCT, the mechanical behaviour of the first and second generation of everolimus-eluting BVS at baseline and at 6-month follow-up.

Devices

The BVS 1.0 (Abbott Vascular, Santa Clara, CA, USA) is a balloon expandable device built on a backbone of semi-crystalline poly-L-lactide (PLLA) polymer. The polymer consists of crystalline and amorphous domains. The balance between the crystalline and amorphous fractions and the molecular orientation state of these phases depends on their thermal and deformation history. The platform is coated with the poly-D,L-lactide (PDLLA) copolymer that contains and controls the release of the antiproliferative everolimus (Novartis, Switzerland). Both PLLA and PDLLA are fully bioresorbable. The strut thickness is 150 μm and the struts are distributed as circumferential out-of-phase zigzag hoops linked together by three longitudinal bridges between each hoop. The BVS 1.0 design is shown in *Figure 1*.

The manufacturing process the BVS 1.1 (Abbott Vascular, Santa Clara, CA, USA) has been modified to enhance the mechanical strength and mechanical durability of the struts. Moreover, the new design has in-phase zigzag hoops linked by bridges that allow for a more uniform strut distribution, reduce maximum circular unsupported surface area, and provide more uniform vessel wall support and drug transfer.[3] The polymer mass, coating content, amount of drug, and the strut thickness remain the same. The BVS 1.1 design is also shown in *Figure 1*.

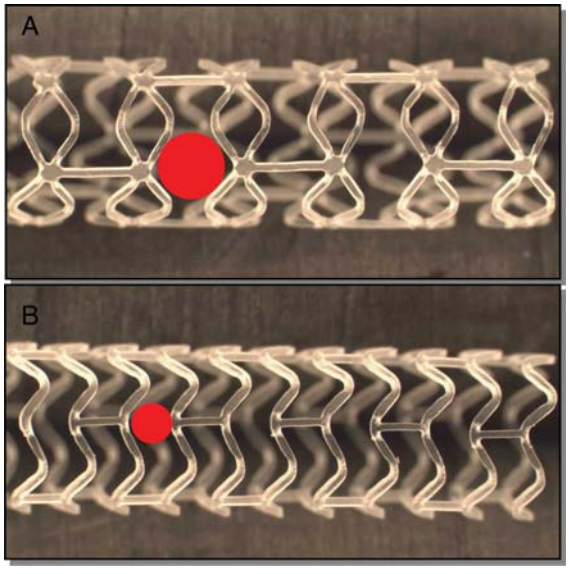

Figure 1 Design of the different bioresorbable vascular scaffold (BVS). (*A*) BVS 1.0 design. The struts are distributed as circumferential out-of-phase zigzag hoops linked together by three longitudinal bridges between each hoop. The maximal circular unsupported surface area is drawn as a red circle. (*B*) BVS 1.1 design. The struts are arranged as in-phase zigzag hoops linked together by three longitudinal bridges. The strut distribution is more uniform and allows the maximal circular unsupported surface area (red circle) to be smaller than in the BVS 1.0.

Treatment procedure

All procedures were performed electively. Lesions were treated with routine interventional techniques that included mandatory pre-dilatation. The study protocol forbade the use of pre-dilatation balloons longer than the pre-specified length of the device (18 mm), and recommended using balloons 0.5 mm smaller in diameter than the reference vessel diameter (RVD). The BVS had to be implanted at a pressure not exceeding the rated burst pressure (16 atmospheres). Post-dilation was allowed at the operator's discretion with shorter balloons than the BVS length and inflated at diameters that fit within the boundaries of the scaffold. Bail-out stenting was also allowed at operator's discretion.

Quantitative angiography analysis

The 2D angiograms were stored in DICOM format and analysed offline by the core lab (Cardialysis, Rotterdam, The Netherlands) using the CASS II analysis system (Pie Medical BV, Maastricht, The Netherlands). In each patient, the treated region and the peri-treated regions (defined by a length of 5 mm proximal and distal to the device edge) were analysed. The following quantitative coronary angiography (QCA) analysis parameters were measured: computer-defined minimal luminal diameter (MLD), RVD obtained by an interpolated method, and percentage of diameter stenosis (DS). Late loss was defined as the difference between MLD post-procedure and MLD at follow-up.[8]

Optical coherence tomography acquisition

In the ABSORB Cohort A, baseline and follow-up OCT acquisition was executed with an M2 Time-Domain System (LightLab Imaging, Westford, MA, USA) using the balloon occlusion method. The occlusion balloon Helios (Goodman, Japan) was advanced distal to the treated region over a conventional angioplasty guidewire of 0.014″. Then, the conventional guidewire was replaced by the OCT ImageWire (LightLab Imaging, Westford, MA, USA) and the occlusion balloon catheter was positioned proximal to the segment of interest. Pullback of the ImageWire was performed with automated pullback at 1 mm/s and 15.6 frames/s during the occlusion of the artery by the balloon at low pressure (0.5–0.7 atm), and during simultaneous flushing of the vessel distal to the occlusion with lactated Ringer's solution at 37°C (flow rate 0.8 mL/s).

In ABSORB Cohort B, the baseline and follow-up OCT acquisitions were performed with the C7 XR Fourier-Domain System (LightLab Imaging, Westford, MA, USA) without occluding the coronary artery. In these cases, a conventional wire was placed distal to the segment of interest. Then the OCT imaging catheter (RX ImageWire II; LightLab Imaging, Westford, MA, USA) was advanced distally to the treated region. Removal of the conventional wire was left to the operator's discretion. The pullback was performed during a continuous injection of 3 mL/s of contrast medium (Iodixanol 370, Visipaque, GE Health Care, Cork, Ireland) injected at a maximum pressure of 300 psi through the guiding catheter using an injection pump. In this case, the automated pullback rate was 20 mm/s and the frame rate was 100 images/s.

The resolution of both OCT systems is exactly the same (15–20 μm of lateral resolution and 15–20 μm of axial resolution).[9]

Optical coherence tomography analysis

The OCT measurements were performed with proprietary software for offline analysis (LightLab Imaging, Westford, MA, USA). Adjusting for the pullback speed, the analysis of contiguous cross-sections was performed at each 1 mm longitudinal intervals within the treated segment.

The monochromatic peak wavelength of the OCT is differently reflected, refracted, and absorbed by the polymeric or metallic struts. A great deal of the OCT light energy is transmitted through the polymeric struts, such that only part of it is reflected at the endoluminal and abluminal sides of the struts generating a visible optical frame border; the core of the polymeric struts is imaged as a black square at baseline. As a consequence, the vessel wall is easily imaged through the struts without any major signs of shadowing (*Figure 2*). Thus, OCT analysis of the BVS has several advantages over that of metallic stents. First, at baseline, the vessel wall/lumen and its luminal area can be readily measured behind the polymeric struts. At follow-up, most of the struts are fully covered and embedded in the vessel wall and the luminal area can be drawn with an automated detection algorithm available in the Light Lab proprietary software; manual corrections are performed if necessary. Second, since polymeric struts are accurately imaged at baseline, the device area can be obtained manually by joining the middle point of each consecutive strut around the circumference. In frames with only a few struts, the BVS area was adjusted to follow the lumen area in the regions where its contour was outside the lumen area. At follow-up, the BVS area was also measured by joining the middle point of the struts (*Figure 3*).

Device shrinkage is defined as the decrease over time of the device area with respect to the area measured immediately after the deployment.[10,11] Absolute late shrinkage has been measured as the difference between the mean BVS area at baseline minus the mean BVS area at follow-up. Relative late shrinkage has been measured as: [(absolute late shrinkage)/baseline mean BVS area] × 100 (*Figure 3*).

In case of incomplete scaffold/strut apposition (ISA), the area between the backside of the struts and the vessel wall has been measured as ISA area. The neointimal area (NIA) has been measured at follow-up as: BVS area – (Lumen Area – ISA area). The neointimal thickness (NIT) has been measured at follow-up with the 'thickness ruler' tool from the endoluminal border of the black strut core to the lumen.

Moreover, a qualitative assessment of the appearance of polymeric struts has been obtained at follow-up. Basically, the struts were classified as preserved box, open box, dissolved bright box, and dissolved black box in order of decreasing reflectivity (*Figure 4*).[1] The kappa index to detect the four types of strut appearance was 0.58.[12] Strut tissue coverage was assessed qualitatively when clear neointimal tissue covered the polymeric strut.

Intra-vascular ultrasound acquisition and analysis

The scaffolded segments were examined with phased array IVUS catheters (EagleEye; Volcano Corporation, Rancho Cordova, CA, USA) with an automated pullback at 0.5 mm/s. Lumen area was measured with a validated computer-based contour detection programme (CURAD BV, Wijk bij Duurstede, The Netherlands) that allows for semi-automatic detection of lumen.[13]

Statistical analysis

Normality distribution of continuous variables was explored with the Kolmogorov–Smirnov test. All continuous variables had normal distribution and have been expressed as means and 1 standard deviation (SD). Categorical variables are presented as counts (%). Paired comparisons of continuous variables within groups between the different time points were done by the Wilcoxon's signed rank test. Comparison of continuous variables between Cohorts A and B has been made using the U-Mann–Whitney test. Comparisons of absolute differences

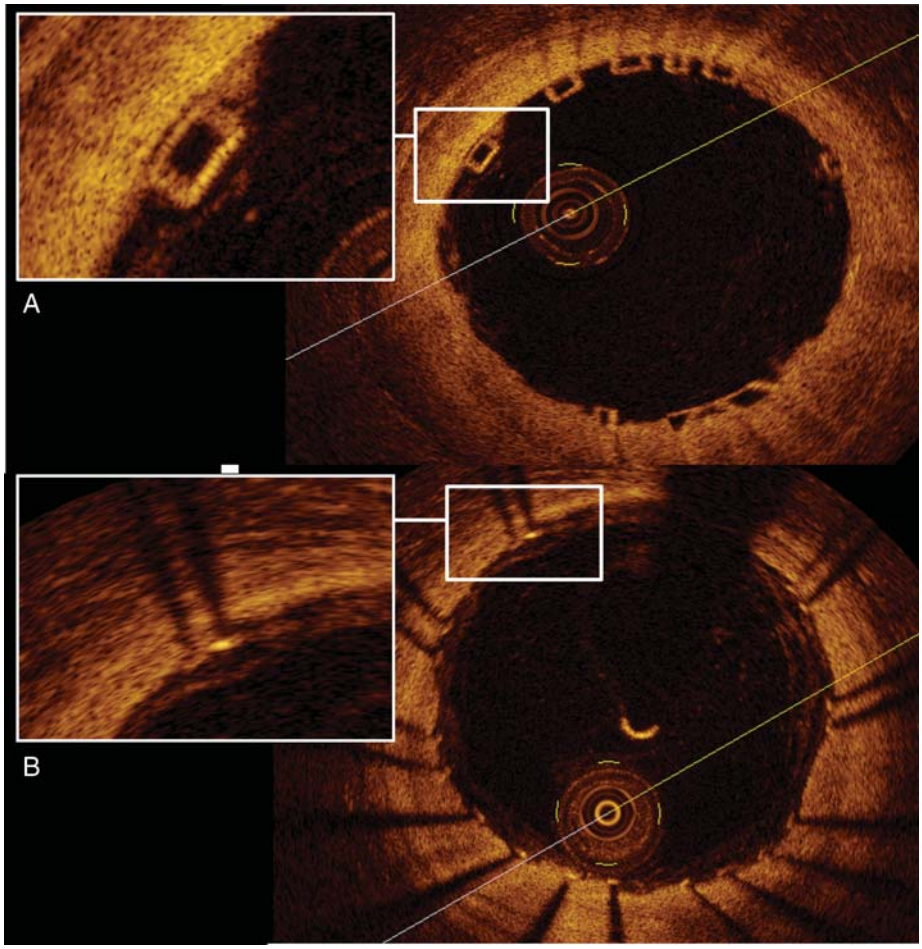

Figure 2 Optical coherence tomography (OCT) imaging of the bioresorbable scaffolds and metallic platform stents. (*A*) Bioresorbable vascular scaffold imaged with OCT. The strut appearance is translucent and allows a perfect imaging of the vessel wall. (*B*) Metallic platform stent imaged with OCT. The metallic struts are opaque to the OCT light and produce the typical shadow into the vessel wall.

between baseline and follow-up have also been made with the U-Mann–Whitney test. Comparisons of categorical variables between groups have been made using the Chi-square test or the Fisher test when one of the cells had less than five events. A two-sided *P*-value ≤ 0.05 was considered statistically significant. All the statistics have been performed with the SPSS 15.0 version for Windows (IL, US).

Results

Study population

A total of 13 lesions in 13 patients had baseline and follow-up OCT imaging in the ABSORB Cohort A study.[1] One of these patients underwent a non-ischaemia driven target lesion revascularization treated with a metallic platform stent at Day 42. The OCT imaging at that time showed strut discontinuation with attached thrombi probably due to overstretching of the BVS during implantation.[7] This patient has not been included in the present study. In the ABSORB Cohort B study, 28 patients with scheduled imaging control at 6-month follow-up were studied with OCT at baseline. Two of them were excluded due to the sub-optimal quality of the imaging, and of the remaining 26 patients, 13 were imaged with the M3 OCT system and 13 were imaged with the OCT C7. None of the 13 patients imaged with the M3 system needed an unscheduled angiography and all of them were studied with OCT at 6 months. One patient imaged with the C7 system presented with a symptomatic peri-procedural myocardial infarction at the index procedure secondary to an occlusion of a small diagonal after the implantation of the BVS in the left anterior descending. This patient refused invasive imaging at 6-month follow-up. Finally, 24 patients were included in the present study: 12 were treated with the BVS 1.0 and 12 were treated with the BVS 1.1. None of those patients had BVS fractures at baseline or 6-month follow-up.

The baseline clinical characteristics are shown in *Table 1*. Both groups were similar in gender and age. There was a trend toward lower percentage of hypercholesterolaemia (72.7 vs. 100.0%; $P = 0.06$) and prior acute myocardial infarction (8.3 vs. 41.7%; $P = 0.06$) in the BVS 1.0 than in the BVS 1.1 group, respectively. There was a significant difference in the smoking status favouring the BVS 1.1 group (33 vs. 0%, respectively; $P = 0.03$).

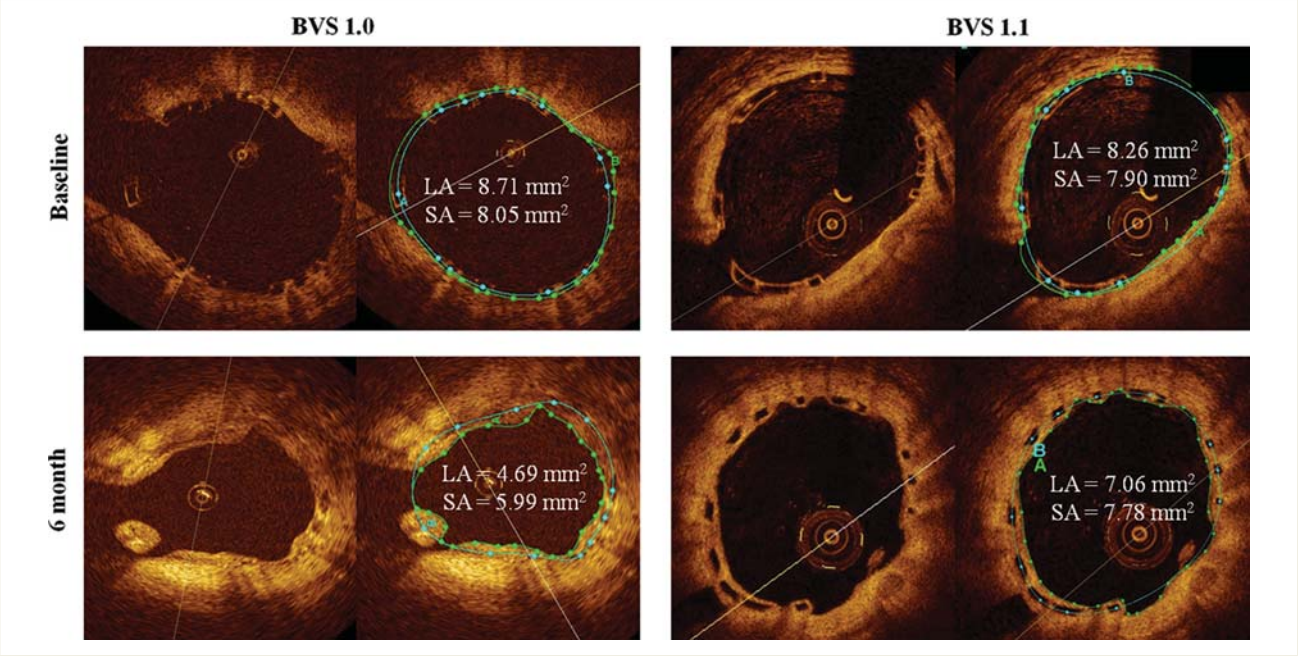

Figure 3 Late shrinkage assessment. Optical coherence tomography (OCT) imaging of the BVS 1.0 and 1.1. At baseline, the scaffold area (SA; blue line) is usually drawn into the luminal area (LA; green line). At follow-up, the neointima covers the polymeric struts and then, the scaffold area usually is drawn outside of the luminal area. The absolute late shrinkage for the BVS 1.0 is 2.06 mm^2 (relative shrinkage of 25.6%) and for the BVS 1.1 is 0.12 mm^2 (relative shrinkage of 1.5%).

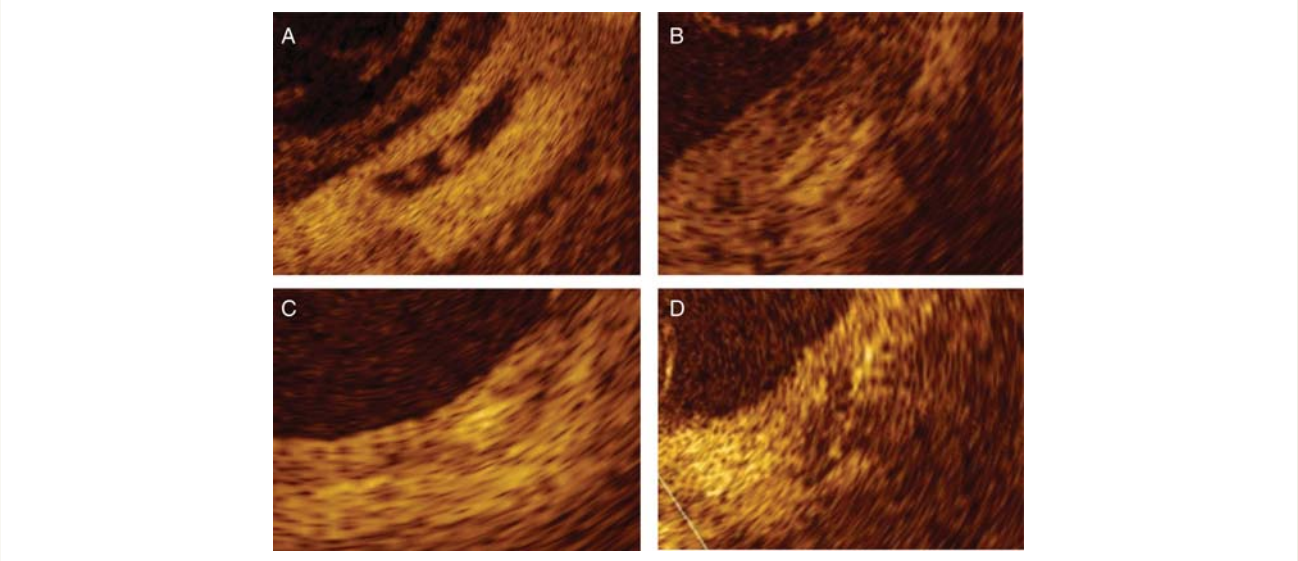

Figure 4 Strut appearance of the bioresorbable vascular scaffold at follow-up. (*A*) Preserved box appearance: sharp defined, bright reflection borders with preserved box-shaped appearance; strut body shows low reflection; (*B*) open box: luminal and abluminal long-axis borders thickened bright reflection; short-axis borders not visible; (*C*) dissolved bright box: partially visible bright spot, contours poorly defined; no box-shaped appearance; (*D*) dissolved black box: black spot, contours poorly defined, often confluent; no box-shaped appearance.

A total of 11 patients in ABSORB Cohort A were treated with a BVS 1.0 of 3 × 12 mm and 1 was treated with a BVS 1.0 of 3 × 18 mm. All patients of the ABSORB Cohort B were treated with a BVS 1.1 of 3 × 18 mm.

Quantitative coronary angiography results

Baseline and follow-up angiographic parameters are shown in *Table 2*. Both groups had similar angiographic characteristics at

Table 1 Baseline clinical and angiographic characteristics

	BVS 1.0 ($n = 12$)	BVS 1.1 ($n = 12$)	*P*-value
Male	8 (66.7)	9 (75.0)	0.65
Age (years ± SD)	59.5 ± 8.3	61.2 ± 9.6	0.76
Hypertension	6 (50.0)	7 (58.3)	0.68
Hypercholesterolaemia	8 (72.7)	12 (100.0)	0.06
Diabetes mellitus	1 (8.3)	1 (8.3)	1.00
Smoke	4 (33.3)	0	0.03
Prior MI	1 (8.3)	5 (41.7)	0.06
Prior PCI	2 (16.7)	3 (25.0)	0.62
Clinical indication			0.27
Stable or silent angina	11 (91.7)	9 (75.0)	
Unstable angina	1 (8.3)	3 (25.0)	
Number of vessel disease			0.14
One	12 (100.0)	10 (83.3)	
Two	0	2 (16.7)	
Culprit vessel			0.22
LAD	4 (33.3)	6 (50.0)	
LCX	6 (50.0)	2 (16.7)	
RCA	2 (16.7)	4 (33.3)	
BVS size			<0.01
3 × 12 mm	11 (91.7)	0	
3 × 18 mm	1 (8.3)	12 (100.0)	

Values are expressed as count (%), except for age.
MI, myocardial infarction; PCI, percutaneous coronary intervention; LAD, left anterior descending; LCX, left circumflex; RCA, right coronary artery; BVS, bioresorbable vascular scaffold.

pre-implantation. Patients treated with the BVS 1.0 tended to have a larger RVD than patients treated with the BVS 1.1 (2.95 vs. 2.69 mm; $P = 0.14$).

At 6-month follow-up, patients treated with the BVS 1.0 had a significant decrease in MLD (angiographic late loss) of 0.43 mm ($P = 0.01$), whereas a non-significant 0.08 mm decrease was seen in those treated with the BVS 1.1. The difference in late loss between the BVS 1.0 and 1.1, although numerically appreciable, failed to reach statistical significance at 6 months ($P = 0.07$). The serial individual changes in MLD between baseline and follow-up are shown in *Figure 5*.

Optical coherence tomography results

Baseline and follow-up quantitative OCT and IVUS findings are shown in *Table 3*. Both groups had similar OCT findings at baseline after the deployment of the BVS. At 6 months, the BVS 1.0 had a significantly higher late shrinkage than the BVS 1.1 (absolute shrinkage of 0.98 vs. 0.07 mm^2 and relative shrinkage of 13.0 vs. 1.0%, respectively; $P = 0.01$). Neointimal area was significantly higher with the BVS 1.0 when compared with the BVS 1.1 (1.44 vs. 0.87 mm^2, respectively; $P < 0.01$). NIH was also larger in the BVS 1.0 than in the BVS 1.1 (166.0 vs. 76.4 μm; $P < 0.01$). These findings at 6 months caused a significantly higher reduction in mean lumen area (relative difference of 35.1 vs. 16.1%; $P < 0.01$) and in minimal luminal area (47.0 vs. 20.7%; $P < 0.01$) with the BVS 1.0 than with the BVS 1.1 as assessed by OCT. Serial individual changes of the BVS area and of the minimal lumen area as assessed by OCT are shown in *Figure 5*. The ISA area of the BVS 1.0 at 6 months increased significantly with respect to the baseline (0.10 mm^2; CI 95%: from −0.02 to 0.21 mm^2; $P = 0.04$), while the ISA area of the BVS 1.1 remained unchanged (0.02 mm^2; −0.18 to 0.22 mm^2; $P = 0.26$).

A total of 662 struts of the BVS 1.0 and 1575 of the BVS 1.1 were detected at baseline. After deployment, all struts appear as preserved box in both BVS devices. At follow-up, 620 struts and 1639 struts were analysed. The strut appearance of the BVS 1.0 showed substantial changes in appearance: at 6 months struts had changed from 100% preserved black box to 29.7% open box, 51.4% dissolved bright box, 16.0% dissolved black box, and only 2.9% were preserved black box. For the BVS 1.1, all struts maintained a preserved black box appearance at 6 months ($P < 0.01$). Uncovered struts were less frequent in the BVS 1.0 (1.1%) than in the BVS 1.1 (5.3%) ($P = 0.01$).

Intravascular-ultrasound results

IVUS results are shown in *Table 3*. The reduction in mean lumen area was larger with the BVS 1.0 than with the BVS 1.1 (12.71 vs. 6.93%), but this difference was not statistically significant ($P = 0.17$). The reduction in minimal lumen area was significantly larger with the BVS 1.0 than with the BVS 1.1 (22.83 vs. 4.81%; $P < 0.01$).

Reproducibility of optical coherence tomography measurements

The scaffold area reproducibility using our method has been assessed specifically for our study. Two independent analysts measured the scaffold area in 100 images at follow-up. After 1 week, one of the analysts re-analysed the same frames. The inter-observer R^2 for repeated measures was 0.88 and the intraobserver R^2 was 0.98.

Discussion

The main findings of our study are: (i) the BVS 1.1 does not show late shrinkage at 6 months with respect to the baseline scaffold area; (ii) the BVS 1.0 has higher neointimal response and higher in-scaffold area obstruction than the BVS 1.1; (iii) these changes resulted in a higher OCT and IVUS luminal losses and angiographic late loss in the BVS 1.0 than in the BVS 1.1; (iv) the overall strut appearance at 6-month follow-up is dramatically different between the two generations of BVS, which may reflect differences in the polymer's interaction with light, arising from differences in microstructure and its degradation.

A pre-clinical animal study involving histological samples at differing time points divided the evolution process of the BVS into two parts:[12] first, the BVS resorption process, which consists of the disappearance of the polymeric PLA and the subsequent

Table 2 Quantitative coronary angiography findings at baseline and 6-month follow-up

BVS	Pre-deployment	Post-deployment	6-month FU	Difference post –pre (CI 95%)	*P*-value*	Difference post – 6 m FU (CI 95%)	*P*-value**	*P*-value†
QCA								
Lesion length (mm)[a]								
BVS 1.0	9.86 (3.46)	10.34 (1.70)	10.17 (2.20)	−0.48 (−2.90 to 1.94)	0.18	0.18 (−0.26 to 0.61)	0.64	0.93
BVS 1.1	8.99 (2.89)	17.08 (1.12)	16.08 (1.48)	−8.09 (−9.82 to −6.35)	<0.01	1.00 (−0.16 to 2.16)	0.13	
RVD (mm)								
BVS 1.0	2.95 (0.38)	3.03 (0.39)	2.87 (0.41)	0.08 (−0.10 to 0.26)	0.31	0.16 (0.01 to 0.31)	0.04	0.24
BVS 1.1	2.69 (0.35)	2.64 (0.23)	2.53 (0.22)	−0.05 (−0.21 to 0.11)	0.70	0.11 (0.02 to 0.20)	0.03	
MLD (mm)								
BVS 1.0	1.13 (0.30)	2.46 (0.38)	2.03 (0.30)	1.32 (1.03 to 1.62)	<0.01	0.43 (0.13 to 0.73)	0.01	0.07
BVS 1.1	1.23 (0.44)	2.26 (0.28)	2.18 (0.25)	1.03 (0.69 to 1.37)	<0.01	0.08 (−0.14 to 0.30)	0.24	
DS (%)								
BVS 1.0	60.8 (13.4)	18.6 (9.4)	27.8 (16.0)	−42.3 (−50.8 to −33.7)	<0.01	−9.3 (−18.7 to 0.2)	0.07	0.24
BVS 1.1	57.6 (13.1)	14.7 (7.5)	15.7 (9.3)	−42.9 (−50.9 to −35.0)	<0.01	−1.0 (−5.5 to 3.5)	0.66	

Data are expressed as mean (SD).
QCA, quantitative coronary angiography; BVS, bioresorbable vascular scaffold; FU, follow-up; RVD, reference vessel diameter; MLD, minimal lumen diameter; DS, diameter stenosis.
[a]Lesion length at post-procedure and at follow-up has been measured between the platinum markers of the BVS.
*Paired comparison between pre- and post-deployment within each group.
**Paired comparison between post-deployment and follow-up within each group.
†Comparison of the difference post-deployment—follow-up between the two groups. Comparison between groups at pre-deployment and post-deployment were non-significant ($P > 0.10$).

filling of the strut voids with proteoglycan material; second, the BVS integration process, which consists of the formation of organized tissue with connective cells and connective extracellular matrices replacing the polymeric and the proteoglycan material. In the same study, the strut appearance as assessed by OCT was compared with matched histological sections.[12] At 24 months, all the struts were discernible by OCT and 80.4% of them were classified as having the preserved box appearance (similar to the BVS 1.1 at 6 months). At that point of time, matched histological samples showed that almost all the strut footprints were occupied by proteoglycans and the analysis with gel permeation chromatography did not find traces of the polymeric material. This demonstrated that the polymer was already resorbed at that time, and therefore OCT imaging was not able to assess the resorption process. At 3- and 4-year follow-up, almost all the struts were not discernible and the few observed struts were classified as a dissolved bright or dissolved black box (similar to the BVS 1.0 at 6 months). There was poor correlation of these types of OCT strut appearance with the particular patterns observed on histology. But, the indiscernible struts and the dissolved black box appearance as assessed by OCT were observed as circumscribed regions of dense connective tissue with low cellularity on histology. Therefore, as assessed by OCT, the most advanced resorption/integration states were characterized as: (i) observation of other types of strut appearance rather than the preserved box; and (ii) the reduction of discernible struts over time jointly with the observation of a dissolved black box strut appearance.[12]

In our study, the number of discernible struts of the BVS 1.1 was slightly lower at baseline than at follow-up (1575 vs. 1639, respectively; $P = 0.06$). At 6 months, the strut appearance was 'preserved' in all the patients. In contrast, the number of discernible struts of the BVS 1.0 was higher at baseline than at follow-up (662 vs. 620, respectively; $P = 0.05$) and at 6 months, only 2.9% of the discernible struts had a preserved box appearance. The correlation of our findings with the animal study shows that the BVS 1.0 had a more advanced resorption/integration state than the BVS 1.1 at 6 months. Our hypothesis is that this faster resorption/integration state is the main cause of the higher late shrinkage and greater neointimal response of the BVS 1.0 compared with the BVS 1.1.

Late shrinkage is a phenomenon resulting from the loss of structural integrity of the polymeric scaffold in conjunction with fatigue and constrictive remodelling of the vessel in the first months following the vessel injury. Loss of structural integrity is an inevitable part of the resorption process of these polymeric devices. The poly-L-lactic acid (PLLA) polymer has a lifecycle which can be divided in five

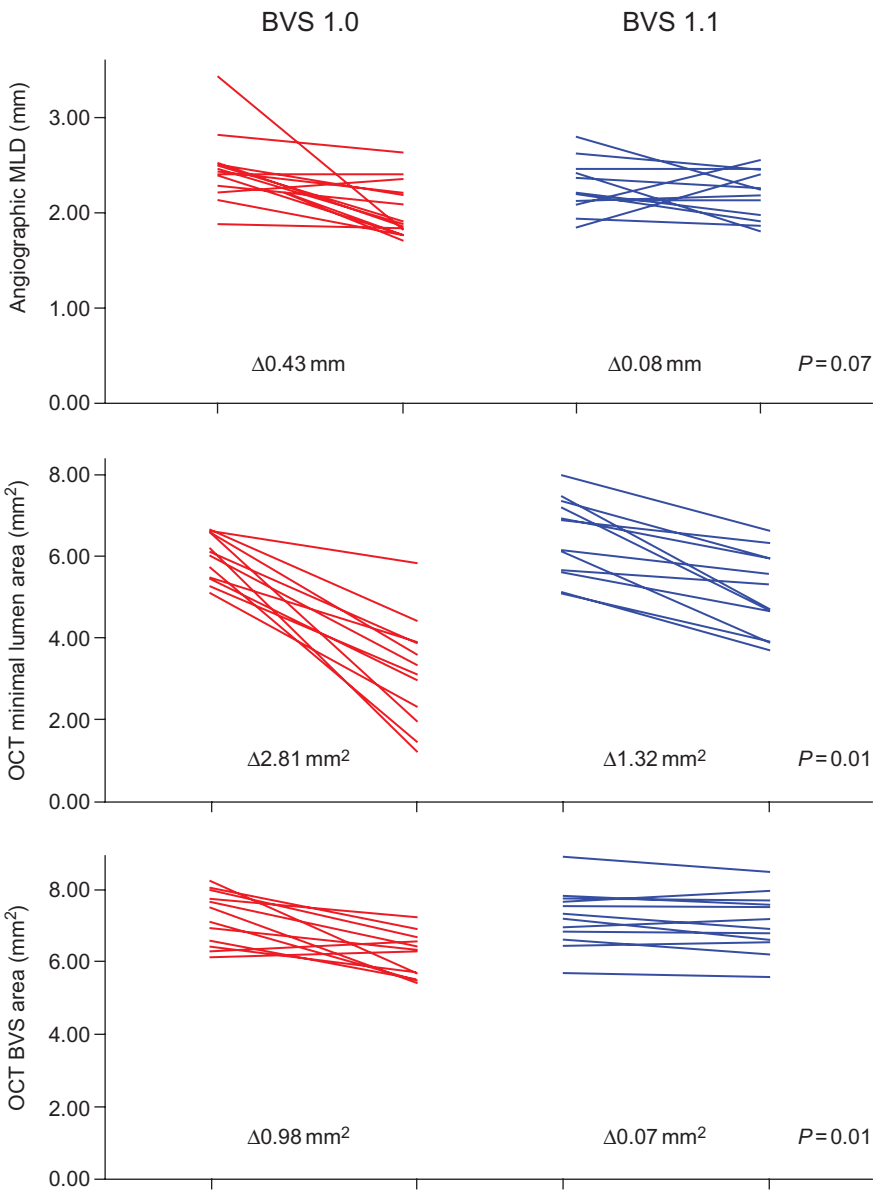

Figure 5 Serial changes in angiographic late lumen loss, BVS area (late shrinkage) and minimal lumen area as assessed by optical coherence tomography.

phases.[14] First, immediately after the deployment, the polymer absorbs water from blood and surrounding tissues. Second, the long chains of PLLA degrade by hydrolysis into smaller chains without affecting the device's structure. Third, the hydrolysis process continues and causes a loss in integrity, with fragmentation of the struts and loss of radial strength. Fourth, soluble monomeric anions dissolve into the intercellular fluid and microparticles of less than 2 μm may be phagocyted by the macrophages; manifesting in mass loss and bioresorption. Finally, the soluble L-lactate is converted into pyruvate, which enters the Krebs cycle, being eventually converted into carbon dioxide and water. The initial degradation process of the PLLA semi-crystalline polymer depends on the length of the polymers chain (molecular weight), the hydrophilicity, and the degree of crystallinitiy. In BVS 1.1, initial degradation rate (i.e. losses in molecular weight leading to structural degradation) has been reduced through changes in the manufacturing process. This slower degradation allows for maintenance of the radial strength over months following the implantation.

The second cause of late shrinkage is the constrictive remodelling of the treated vessel in the first few months after implantation. In the era of balloon angioplasty, more than 70% of the restenotic process was attributed to negative remodelling of the vessel in the treated segment, and less than 30% was done to neointimal growth.[15] In the metallic stent era, late lumen loss within the stent correlated strongly with tissue growth ($r = 0.975$), eliminating negative remodelling as the common cause of restenosis.[16,17] Thus, the key question for intracoronary bioresorbable scaffolds is for how long radial strength (i.e. scaffolding) must be maintained

Table 3 Quantitative optical coherence tomography and intravascular ultrasound findings at baseline and 6-month follow-up

BVS (n = 12 vs. 12)	Baseline (post-deployment)	6-month FU	Absolute difference between BL and FU (CI 95%)	Relative difference between BL and FU (%)	*P*-value*	*P*-value**
OCT						
Mean luminal area (mm^2)						
1.0 BVS	7.63 (0.79)	4.94 (1.10)	2.69 (1.99–3.39)	35.07 (13.31)	<0.01	<0.01
1.1 BVS	7.67 (0.94)	6.44 (0.93)	1.23 (0.89–1.57)	16.09 (6.48)	0.01	
Minimal luminal area (mm^2)						
1.0 BVS	5.99 (0.57)	3.19 (1.28)	2.81 (2.03–3.59)	46.97 (19.67)	<0.01	<0.01
1.1 BVS	6.32 (0.96)	5.01 (0.97)	1.32 (0.83–1.80)	20.65 (10.94)	<0.01	
Mean BVS area (mm^2)						
1.0 BVS	7.18 (0.73)	6.20 (0.64)	0.98 (0.42–1.54)	12.95 (11.70)	0.01	0.01
1.1 BVS	7.21 (0.82)	7.14 (0.84)	0.07 (−0.10 to 0.24)	0.97 (3.73)	0.37	
Minimal BVS area (mm^2)						
1.0 BVS	5.82 (0.60)	4.75 (0.83)	1.07 (0.49–1.66)	17.90 (14.26)	<0.01	0.01
1.1 BVS	6.21 (0.98)	6.00 (0.85)	0.21 (−0.14 to 0.56)	2.81 (8.11)	0.29	
ISA area (mm^2)						
1.0 BVS	0.14 (0.25)	0.22 (0.31)	−0.10 (−0.21 to 0.02)	−36.36 (10.33)	0.04	0.88
1.1 BVS	0.15 (0.30)	0.17 (.18)	−0.02 (−0.22 to 0.18)	−11.76 (15.35)	0.26	
NIA (mm^2)						
1.0 BVS	NA	1.44 (0.32)	NA	NA	NA	<0.01[a]
1.1 BVS	NA	0.87 (0.22)	NA	NA	NA	
NIT (mm)						
1.0 BVS	NA	0.17 (0.04)	NA	NA	NA	<0.01[a]
1.1 BVS	NA	0.08 (0.02)	NA	NA	NA	
In-device area obstruction (%)						
1.0 BVS	NA	23.62 (6.55)	NA	NA	NA	<0.01[a]
1.1 BVS	NA	12.28 (3.38)	NA	NA	NA	
IVUS						
Mean luminal area (mm^2)						
1.0 BVS	6.84 (0.74)	5.94 (0.67)	0.90 (0.43–1.37)	12.71 (9.89)	<0.01	0.17
1.1 BVS	6.69 (0.81)	6.20 (0.76)	0.47 (0.24–0.69)	6.93 (4.68)	<0.01	
Minimal luminal area (mm^2)						
1.0 BVS	5.75 (0.52)	4.41 (0.70)	1.34 (0.83–1.84)	22.83 (12.73)	<0.01	<0.01
1.1 BVS	5.51 (0.78)	5.15 (0.73)	0.28 (−0.01 to 0.57)	4.81 (7.20)	0.09	

Data are expressed in mean (SD).
OCT, optical coherence tomography; IVUS, intravascular ultrasound; ISA, incomplete scaffold/strut apposition; NIA, neointimal area; NIT, neointimal thickness; NA, not applicable.
Comparison of the OCT and IVUS findings at baseline between groups showed no significant differences.
[a]Comparison of the neointimal hyperplasia (NIA and NIT) and in-device area obstruction at follow-up between groups.
**P*-value between baseline and follow-up within groups.
***P*-value comparing the absolute differences between groups.

to avoid constrictive remodelling. In a cohort of patients consecutively re-catheterizated at 1, 2, 3, and 4 months, Serruys *et al.*[18] demonstrated that the restenotic process after balloon angioplasty ceases to progress after 4 months. It is possible that after this time, scaffolding is no longer needed, and the structural degradation and bioresorption processes can commence.

It is uncertain whether the constrictive remodelling is more focused in the regions of the vessel with more plaque burden or is equally distributed. This can affect the results of our study due to the differences in the BVS lengths according to the lesion length. The lesion length prior to the implantation was similar in both groups (around 9–10 mm), but the device length as assessed by QCA at post-deployment was significantly higher in the BVS 1.1 than in the BVS 1.0 (17.08 vs. 10.34 mm; $P < 0.01$). This difference resulted from the fact that all patients treated in the ABSORB Cohort B study received a single size device (3 × 18 mm), while in the ABSORB Cohort A there were two different sizes (3 × 12 and 3 × 18 mm). A sub-analysis of the 12 central millimetre

of the scaffold imaged by OCT (that part of the scaffold is more likely to be located at the nadir of the narrowing) in the patients treated with a 3 × 18 mm showed that the mean scaffold area at baseline and at 6-month follow-up was 7.18 and 6.19 mm^2 with the BVS 1.0 (relative shrinkage of 13.09%) and 7.14 and 7.10 mm^2 with the BVS 1.1 (relative shrinkage of 0.50%); $P = 0.01$.

Until now, four different fully bioresorbable scaffolds have been tested in humans. The polymeric PLLA non-drug-eluting Igaki-Tamai device was the first fully bioresorbable scaffold used in humans. The IVUS analysis did not show bioresorption of the polymeric struts at 6 months and this absence of ultrasonic changes in struts was parallel to the absence of scaffold shrinkage. This device presented a target vessel revascularization of 6.7% at 6 months and a low rate of major cardiac events at 10 years.[19,20] Conversely, the PROGRESS-AMS magnesium platform non-drug-eluting bioresorbable scaffold had a rapid resorption which was complete at 4-month follow-up. This swift resorption produced an important reduction of the lumen (60% of the late lumen loss) and a high incidence of restenosis (47.5% assessed by QCA).[21] The REVA device is a poly (iodinated desaminotyrosyl-tyrosine ethyl ester) carbonate non-drug-eluting scaffold. The closed design and the lifecycle of the carbonate provide enough radial strength during the first 3 months following the implantation without appreciable shrinkage. However, focal mechanical failures driven by polymer embrittlement led to a high rate of TLR (66.7%) between 4- and 6-month follow-up.[22] Finally, the IDEAL™ Poly (Anhydride Ester) Salicylic acid sirolimus-eluting device has been tested in only 11 patients.[23]

The shrinkage phenomenon observed in the BVS 1.0 was linked to a significant increase of the ISA area with respect to baseline and with higher neointimal response with respect to the BVS 1.1. The increasing of the ISA area with the BVS 1.0 can be explained by the scaffold shrinkage itself. At baseline, 95% of the struts were apposed or aligned, while in the follow-up only 93% of the struts were apposed to the vessel wall. Moreover, less than 10% of the malapposed struts at baseline were resolved at follow-up.[1] The NIA measured in this population was significantly different between the two generations of BVS (1.44 mm^2 for the BVS 1.0 vs. 0.87 mm^2 for the BVS 1.1). In-scaffold area obstruction was also different between BVS 1.0 and 1.1 (23.6 vs. 12.3%, respectively). The significantly lower neointimal response of the BVS 1.1 with respect to the BVS 1.0 has no clear explanation. Both generations of BVS are built with the same polymer mass, strut thickness, drug, and coating elution and the same amount of drug. One hypothesis is that the loss in scaffold area leads to a decreased efficiency in drug transfer to the vessel wall and thus, a reduction in antiproliferative efficacy. Another hypothesis is that the more accelerated resorption/integration process of the BVS 1.0 compared with the BVS 1.1 could generate a larger neointimal response. Unfortunately, this cannot be assessed by OCT due to the lack of correlation between the different types of strut appearance and the histological findings based on animal studies.[12] An exploratory analysis of the patients treated with the BVS 1.0 in our study relating the NIT measured above the preserved box appearance (0.15 ± 0.04 μm) with the NIT measured above the other types of strut appearance (0.18 ± 0.06) failed to be significant ($P = 0.27$). The same patients treated with the BVS 1.0 studied with OCT at 2 years showed few discernible struts with no measurable neointima. Nevertheless, the mean lumen area increased up to 19% from 6-month to 2-year follow-up.[4] This fact may be a sign of vessel remodelling at the neointimal level but the low number of patients are a clear limitation to this conclusion. This hypothesis will be examined further when the strut appearance of patients treated with the BVS 1.1 changes in future scheduled imaging controls.

The OCT performance of the BVS 1.1 can be compared with some drug-eluting stents (DES). The NIT observed in the BVS 1.1 (0.08 mm) is similar to that seen with the sirolimus-DES (from 0.05 to 0.12 mm) at 6-month follow-up.[24,25] Paclitaxel-DES and zotarolimus-DES showed an NIT of 0.20 and 0.33 mm, respectively.[24] The late shrinkage of metallic DES has not been yet explored with OCT. Using IVUS, the everolimus-DES showed a relative difference in mean stent area of 0.3% at 6-month follow-up.[26] This value is similar to the 1.0% found in our study with the BVS 1.1. Based on this information, the BVS 1.1 presents a similar profile as the metallic DES as assessed by OCT.

In summary, our study represents the first comparison of two generations of bioresorbable devices in terms of late shrinkage, neointimal response, and bioresorption state using the most sophisticated intravascular imaging technique (OCT) and the same methodology for both devices. The OCT findings at 6 months show the improvement of the new generation of BVS with respect to the previous generation. The slower bioresorption process of the BVS 1.1, compared with the BVS 1.0, is the most plausible explanation for the near elimination of the late shrinkage and for the higher inhibition of the neointimal response. Further investigations will be required to assess the preservation of these results after 6-month follow-up for the BVS 1.1. A more advanced bioresorption state can contribute to a very late shrinkage of the device or later neointimal responses.

Limitations

The result of the present analysis must be interpreted with caution as a major limitation of our study is the small number of patients who have been enrolled in a non-randomized comparison. *Figure 5* shows that there is a homogeneous trend of higher late shrinkage and higher loss in minimal lumen area in the BVS 1.0 than in the BVS 1.1. The histogram distribution of the NIA in the two populations also shows this trend of higher neointimal growth in the BVS 1.0 than in the BVS 1.1 (data not shown). This trend, however, is not observed with the angiographic late lumen loss in which one outlier can be influencing the higher late lumen loss in the BVS 1.0. Moreover, two eligible patients imaged at baseline and scheduled for an invasive follow-up at 6 months did not undergo repeat invasive imaging. It is uncertain how this lack of serial imaging in those patients affects the global results of our study. Although the small number of patients, we have used the maximal number of 'historical' cases performed with the BVS 1.0 and imaged with the best available OCT system M2 at that time and compared with the same number of patients of the BVS 1.1 imaged with the best available system nowadays (OCT C7 system).

These differences in OCT systems are inherent to the fact that the ABSORB Cohort A trial was conducted in 2006, when a

balloon occlusive technique was needed due to the lower frame/rate and acquisition speed of the available systems at that time. One *in vitro* study showed less accuracy in the lumen area measurement with lower frame rate and acquisition speed than with higher frame/rate and speed.[27] An *in vivo* study, comparing the non-occlusive and the occlusive technique in the same non-scaffolded native coronary artery, showed systematically smaller mean and minimal lumen areas with the occlusive technique than with the non-occlusive technique (relative differences of 13.2 and 28.2%, respectively).[28] These differences were probably produced by the lack of physiological pressurization of the vessel during the occlusive technique imaging and/or the over-pressurization of the vessel during the contrast infusion of the non-occlusive technique.[28] These differences represent an important limitation of our study because the two different devices were imaged with different OCT techniques (occlusive for the BVS 1.0 and non-occlusive for the BVS 1.1). However, in our study, the baseline and follow-up acquisition were performed using the same imaging technique in each cohort of patients and also, the analysed region is scaffolded by the BVS. The scaffolded region is probably less susceptible to changes in volumetric parameters according to the intravascular pressure. Unfortunately, there is no current information comparing the changes in lumen areas within the scaffolded regions with the two different OCT techniques.

The method of analysis used in our study is slightly different from the current method of OCT measurement of polymeric scaffold. The strut appearance of the BVS 1.0 at 6 months (and probably the appearance of the BVS 1.1 in later controls) does not permit the delineation of the strut contour at the front or backside of the strut. Using the central part of the strut as landmark for measurement is the most reliable method to assess the scaffold area. However, it must be recognized that the neointima area as such determined is an arbitrary entity resulting from the difference between the luminal area and the scaffold area, and does not depict accurately the neointimal tissue that has grown between, on the top and behind the struts either biologically altered in the case of the BVS 1.0 or almost intact in the case of the BVS 1.1.

Finally, the differences in device lengths in the two groups may be favourable to the BVS 1.1 due to a better anchoring in the healthy part of the vessel that can be subjected to a less constrictive modelling of the vessel.

Conclusion

The two generations of the everolimus-eluting bioresorbable vascular scaffold have different OCT findings at 6-month follow-up. The BVS 1.1 has less late shrinkage and less neointimal growth at 6-month follow-up compared with the BVS 1.0. Consequently, less angiographic late loss and less OCT and IVUS luminal losses were observed with the BVS 1.1. A difference in polymer degradation leading to changes in microstructure and reflectivity is the most plausible explanation for this finding.

Conflict of interest: S.W. is a consultant for Abbott, Biosensors, Boston Scientific, Cordis and Medtronic.

Funding

This work was supported by Abbott.

References

1. Ormiston JA, Serruys PW, Regar E, Dudek D, Thuesen L, Webster MW, Onuma Y, Garcia-Garcia HM, McGreevy R, Veldhof S. A bioabsorbable everolimus-eluting coronary stent system for patients with single de-novo coronary artery lesions (ABSORB): a prospective open-label trial. *Lancet* 2008;**371**:899–907.
2. Painter JA, Mintz GS, Wong SC, Popma JJ, Pichard AD, Kent KM, Satler LF, Leon MB. Serial intravascular ultrasound studies fail to show evidence of chronic Palmaz-Schatz stent recoil. *Am J Cardiol* 1995;**75**:398–400.
3. Okamura T, Garg S, Gutierrez-Chico JL, Shin ES, Onuma Y, Garcia-Garcia HM, Rapoza R, Sudhir K, Regar E, Serruys PW. In vivo evalution of stent strut distribution patterns in the bioabsorbable everolimus-eluting device: an OCT ad hoc analysis of the revision 1.0 and revision 1.1 stent design in the ABSORB clinical trial. *EuroIntervention* 2010;**5**:932–938.
4. Serruys PW, Ormiston JA, Onuma Y, Regar E, Gonzalo N, Garcia-Garcia HM, Nieman K, Bruining N, Dorange C, Miquel-Hebert K, Veldhof S, Webster M, Thuesen L, Dudek D. A bioabsorbable everolimus-eluting coronary stent system (ABSORB): 2-year outcomes and results from multiple imaging methods. *Lancet* 2009;**373**:897–910.
5. Kawase Y, Hoshino K, Yoneyama R, McGregor J, Hajjar RJ, Jang IK, Hayase M. In vivo volumetric analysis of coronary stent using optical coherence tomography with a novel balloon occlusion-flushing catheter: a comparison with intravascular ultrasound. *Ultrasound Med Biol* 2005;**31**:1343–1349.
6. Suzuki Y, Ikeno F, Koizumi T, Tio F, Yeung AC, Yock PG, Fitzgerald PJ, Fearon WF. In vivo comparison between optical coherence tomography and intravascular ultrasound for detecting small degrees of in-stent neointima after stent implantation. *JACC Cardiovasc Interv* 2008;**1**:168–173.
7. Onuma Y, Serruys PW, Ormiston JA, Regar E, Webster M, Thuesen L, Dudek D, Veldhof S, Rapoza R. Three-year results of clinical follow-up after a bioresorbable everolimus-eluting scaffold in patients with de novo coronary artery disease: the ABSORB trial. *EuroInterv* 2010;**6**:447–453.
8. Reiber JH, Serruys PW, Kooijman CJ, Wijns W, Slager CJ, Gerbrands JJ, Schuurbiers JC, den Boer A, Hugenholtz PG. Assessment of short-, medium-, and long-term variations in arterial dimensions from computer-assisted quantitation of coronary cineangiograms. *Circulation* 1985;**71**:280–288.
9. Takarada S, Imanishi T, Liu Y, Ikejima H, Tsujioka H, Kuroi A, Ishibashi K, Komukai K, Tanimoto T, Ino Y, Kitabata H, Kubo T, Nakamura N, Hirata K, Tanaka A, Mizukoshi M, Akasaka T. Advantage of next-generation frequency-domain optical coherence tomography compared with conventional time-domain system in the assessment of coronary lesion. *Catheter Cardiovasc Interv* 2009;**75**:202–206.
10. Tanimoto S, Serruys PW, Thuesen L, Dudek D, de Bruyne B, Chevalier B, Ormiston JA. Comparison of in vivo acute stent recoil between the bioabsorbable everolimus-eluting coronary stent and the everolimus-eluting cobalt chromium coronary stent: insights from the ABSORB and SPIRIT trials. *Catheter Cardiovasc Interv* 2007;**70**:515–523.
11. Tanimoto S, Bruining N, van Domburg RT, Rotger D, Radeva P, Ligthart JM, Serruys PW. Late stent recoil of the bioabsorbable everolimus-eluting coronary stent and its relationship with plaque morphology. *J Am Coll Cardiol* 2008;**52**:1616–1620.
12. Onuma Y, Serruys P, Perkins L, Okamura T, Gonzalo N, Garcia-Garcia HM, Regar E, Kamberi M, Powers JC, Rapoza R, van Beusekom H, van der Giessen W, Virmani R. Intracoronary optical coherence tomography (OCT) and histology at 1 month, at 2, 3 and 4 years after implantation of everolimus-eluting bioresorbable vascular scaffolds in a porcine coronary artery model: An attempt to decipher the human OCT images in the ABSORB trial. *Circulation* 2010; Published online ahead of print 25 October 2010.
13. von Birgelen C, de Vrey EA, Mintz GS, Nicosia A, Bruining N, Li W, Slager CJ, Roelandt JR, Serruys PW, de Feyter PJ. ECG-gated three-dimensional intravascular ultrasound: feasibility and reproducibility of the automated analysis of coronary lumen and atherosclerotic plaque dimensions in humans. *Circulation* 1997;**96**:2944–2952.
14. Aalst M, Eenink M, Kruft M, van Tuil R. ABC's of bioabsorption: application of lactide based polymers in fully resorbable cardiovascular stents. *Eurointervention* 2009;**5**(Suppl. F):F23–F27.
15. Mintz GS, Popma JJ, Pichard AD, Kent KM, Satler LF, Wong C, Hong MK, Kovach JA, Leon MB. Arterial remodeling after coronary angioplasty: a serial intravascular ultrasound study. *Circulation* 1996;**94**:35–43.
16. Hoffmann R, Mintz GS, Dussaillant GR, Popma JJ, Pichard AD, Satler LF, Kent KM, Griffin J, Leon MB. Patterns and mechanisms of in-stent restenosis. A serial intravascular ultrasound study. *Circulation* 1996;**94**:1247–1254.

17. Nakamura M, Yock PG, Bonneau HN, Kitamura K, Aizawa T, Tamai H, Fitzgerald PJ, Honda Y. Impact of peri-stent remodeling on restenosis: a volumetric intravascular ultrasound study. *Circulation* 2001;**103**:2130–2132.
18. Serruys PW, Luijten HE, Beatt KJ, Geuskens R, de Feyter PJ, van den Brand M, Reiber JH, ten Katen HJ, van Es GA, Hugenholtz PG. Incidence of restenosis after successful coronary angioplasty: a time-related phenomenon. A quantitative angiographic study in 342 consecutive patients at 1, 2, 3, and 4 months. *Circulation* 1988;**77**:361–371.
19. Tamai H, Igaki K, Kyo E, Kosuga K, Kawashima A, Matsui S, Komori H, Tsuji T, Motohara S, Uehata H. Initial and 6-month results of biodegradable poly-l-lactic acid coronary stents in humans. *Circulation* 2000;**102**:399–404.
20. Nishio S, Kosuga K, Okada M, Harita T, Ishii M, Kawata Y, Takeda S, Takeuchi Y, Hata T, Ikeguchi S. Long term (>10 years) clinical outcomes of the first-in-man biodegradable poly-L-lactic acid coronary stents. Oral presentation. Paris: EuroPCR; 2010.
21. Erbel R, Di Mario C, Bartunek J, Bonnier J, de Bruyne B, Eberli FR, Erne P, Haude M, Heublein B, Horrigan M, Ilsley C, Bose D, Koolen J, Luscher TF, Weissman N, Waksman R. Temporary scaffolding of coronary arteries with bioabsorbable magnesium stents: a prospective, non-randomised multicentre trial. *Lancet* 2007;**369**:1869–1875.
22. Pollman M. Engineering a bioresorbable stent: the REVA programme update. *EuroIntervention* 2009;**5**(Suppl. F):F54–F57.
23. Jabara R. *Poly-anhydridre Basic on Salicylic Acid and Adipic Acid Anhydridre*. Barcelona: EuroPCR; 2009.
24. Guagliumi G, Musumeci G, Sirbu V, Bezerra HG, Suzuki N, Fiocca L, Matiashvili A, Lortkipanidze N, Trivisonno A, Valsecchi O, Biondi-Zoccai G, Costa MA. Optical coherence tomography assessment of in vivo vascular response after implantation of overlapping bare-metal and drug-eluting stents. *JACC Cardiovasc Interv* 2010;**3**:531–539.
25. Matsumoto D, Shite J, Shinke T, Otake H, Tanino Y, Ogasawara D, Sawada T, Paredes OL, Hirata K, Yokoyama M. Neointimal coverage of sirolimus-eluting stents at 6-month follow-up: evaluated by optical coherence tomography. *Eur Heart J* 2007;**28**:961–967.
26. Serruys PW, Ong AT, Piek JJ, Neumann FJ, van der Giessen WJ, Wiemer M, Zeiher A, Grube E, Haase J, Thuesen L, Hamm C, Otto-Terlouw PC. A randomized comparison of a durable polymer Everolimus-eluting stent with a bare metal coronary stent: The SPIRIT first trial. *EuroIntervention* 2005;**1**:58–65.
27. Sawada T, Shite J, Negi N, Shinke T, Tanino Y, Ogasawara D, Kawamori H, Kato H, Miyoshi N, Yoshino N, Kozuki A, Koto M, Hirata K. Factors that influence measurements and accurate evaluation of stent apposition by optical coherence tomography. Assessment using a phantom model. *Circ J* 2009;**73**:1841–1847.
28. Gonzalo N, Serruys PW, Garcia-Garcia HM, van Soest G, Okamura T, Ligthart J, Knaapen M, Verheye S, Bruining N, Regar E. Quantitative ex vivo and in vivo comparison of lumen dimensions measured by optical coherence tomography and intravascular ultrasound in human coronary arteries. *Rev Esp Cardiol* 2009;**62**:615–624.